Use of cold waters geochemistry as a geothermal prospecting tool for hidden hydrothermal systems in Réunion Island

Bhavani Bénard, Vincent Famin, Pierre Agrinier, Pascale Louvat, Geneviève Lebeau, Pierre Burckel

communications earth & environment

ARTICLE

https://doi.org/10.1038/s43247-024-01210-3 OPEN

Use of cold waters geochemistry as a geothermal prospecting tool for hidden hydrothermal systems in Réunion Island

Bhavani Bénard[1,2,3]✉, Vincent Famin[1,2], Pierre Agrinier[1], Pascale Louvat[1,4], Geneviève Lebeau[1,2] & Pierre Burckel[1]

Most untapped high-enthalpy geothermal resources are blind, meaning lacking surface evidence of their existence. The first step in their discovery is to find evidence of hydrothermal activity. Here we apply an approach based on the geochemistry of cold waters, which allowed us to identify evidence of the existence of a hydrothermal system at Piton de la Fournaise volcano (Réunion Island), and constrain its location. This approach uses the concentrations in B, Li, SO_4, F, Mo, P, V, As and HCO_3 and the isotopic ratios $\delta^{13}C$ and $\delta^{11}B$ as geochemical markers of hydrothermal activity that can be used even in waters with extremely low ion content (Electrical conductivity <80 μS/cm), and even when their geochemical composition is mainly controlled by other processes. This noninvasive approach is easy to implement and can be applied wherever the presence of a blind geothermal system is suspected.

[1] Université de Paris, Institut de Physique du Globe de Paris, CNRS, F-75005 Paris, France. [2] Université de La Réunion, Laboratoire GéoSciences Réunion, F-97744 Saint Denis, France. [3] Observatoire Volcanologique du Piton de la Fournaise, Institut de Physique du Globe de Paris, F-97418 La Plaine des Cafres, France. [4] Université de Pau et des Pays de l'Adour, E2S UPPA, CNRS, IPREM, UMR, 5254 Pau, France. ✉email: benard@ipgp.fr

Geothermal development consists in harvesting the energy naturally generated by hydrothermal activity. Geothermal exploration is therefore greatly facilitated by the presence of obvious surface markers of hydrothermal activity such as hot springs or fumaroles. While there are plenty of efficient methods for exploring geothermal systems displaying such evidence, less visible systems prove hard to uncover, thus restraining the development of geothermal energy worldwide. Yet, with the acceleration of climate change from the use of fossil fuels, geothermal energy represents a necessary renewable and local alternative. To address this issue, the scientific community in all Earth-sciences related disciplines has been developing exploration strategies for almost two decades, specifically targeting "hidden" or "blind" geothermal systems, i.e., with no obvious surface evidence of hydrothermal activity[1–7]. For high-enthalpy systems and conventional geothermal use, the first milestone is to determine whether or not there is hydrothermal activity, as it represents the base condition. So far, few approaches have been proposed using water geochemistry. Indeed, the widely used geochemical tools in non-blind systems rely on the study of hot springs and fumaroles, absent in blind systems. Yet, small hydrothermal components are often highlighted in groundwater studies in volcanic environments[8–22] and could therefore theoretically constitute an exploration tool. In most cases the quantification of the hydrothermal contribution is made using anionic mass budgets (Cl, SO_4, HNO_3) but also trace elements concentrations and isotopic ratios that are typically enriched (B, Li, …) or depleted (Se, Ge) or fractionated (δ^7Li, δ^{11}B, δ^{34}S, δ^{13}C, δ^{30}Si) in the hydrothermal fluids compared to the "cold" waters. Only in the recent exploration campaigns in the islands of Hawai'i, unconventional geochemical tools were used on cold groundwaters, whose compositions result mostly from non-hydrothermal processes, which along with other methods proved efficient to evidence the existence of hidden geothermal systems[3]. In these ocean island volcanoes, it is assumed that strong lateral groundwater flows conceal the rise of hot fluids and that to some extent, these hot fluids are diluted in a wider hydrogeological network. While bulk geochemical data for these "mixed" groundwaters fall into the range of expected values for "pure" groundwaters, by comparing the temperatures, Cl/Mg concentration ratios and SiO_2 concentrations between groundwaters samples harvested at the scale of the islands, Lautze et al.[3] were able to decipher geochemical anomalies associated with hydrothermal activities in some samples. Ferguson[23] showed that these waters also displayed anomalous He content and R/Ra ratios. These studies touch upon the possibilities of using geochemical markers of hydrothermal activity in cold groundwaters as an exploration tool for the first stage of geothermal exploration in blind systems, which is the approach we develop here on a larger scale.

We chose the Piton de la Fournaise volcano (Réunion Island) as our natural laboratory. This ocean island volcano displays no visible surface indicators of hydrothermal activity despite an ongoing frequent volcanic activity. As in other blind systems, geophysical studies as well as studies on the geochemistry of soil gas have been conducted for geothermal exploration, which concluded to the possible presence of hydrothermal systems at different locations in the volcanic edifice[24]. Additionally, in unrelated studies, observed peculiarities in the Radon content and the isotopic composition (δ^{13}C and δ^{11}B) of several cold groundwater samples of the massif have tentatively been attributed to the presence of magmatic fluids[25–27]. Therefore, to date, the presence of a hidden geothermal system on this volcano, although strongly suggested, is still questioned, making it an ideal candidate for the development of new exploration strategies such as the study of the chemistry of cold waters, as a complementary approach to the other methods. Here, we acquired a large dataset both in terms of samples and analyzed parameters to try and find markers of a hydrothermal signature and fit them in a hydrogeological circulation model. We sampled 80 cold springs, groundwater wells, rivers and streams on the volcanic massif (Fig. 1A) and analyzed them for major and trace elements concentrations and δ^{11}B and δ^{13}C isotopic ratios.

We show that high temperature water-rock interaction and/or dissolution of magmatic gases can be evidenced in Piton de la Fournaise waters by the relative enrichments in As, Rb, P, V, Mo, Sb, F, Li, SO_4, HCO_3 and B, as well as by the isotopic ratios δ^{11}B and δ^{13}C. With these geochemical markers of hydrothermal activity, we built a unique index that measures the relative probability of the presence of a hydrothermal component in waters. The spatial distribution of waters with the most evidence of hydrothermal activity indicates that a caldera fault system surrounding the Plaine des Sables region is a preferential pathway for rising hydrothermal fluids. These results are consistent with previous geophysical exploration studies which identified a dense body and a conductive layer as a potential geothermal resource in this region[24,28,29].

Results and discussion

Identifying geochemical markers of hydrothermal activity. At Piton de la Fournaise, the aquifer system is unconfined and constituted by stacked lava flows[30]. Lavas are transitional between the tholeiitic and alkaline fields and have a range of compositions from picrite to trachyandesite, with a large majority of aphyric basalt[31–33]. At a regional scale, permeability is decreasing from the surface to the depth of the edifice, the deeper units being older and thus more affected by secondary mineralization processes. These oldest units act as a wall for interconnected groundwater flows of regional extent with waters going from the inner to the outer part of the edifice. Preferential pathways or isolated circulations can result from local discontinuities in the stacked lava flows, such as permeable paleo-valleys and less permeable paleosoils[30,34,35]. Because the aquifer system is interconnected and of regional extent, we expect that the presence of a hydrothermal system would result in a dilution of thermal waters into the aquifer system, as in Hawai'i[3].

There are no resurgences of waters displaying a strong thermal component at Piton de la Fournaise, which was confirmed by our extensive fieldwork. From their interaction with hot rocks, hot fluids, and magmatic gases, thermal waters are hot and/or acidic and/or with a high total dissolved solid content. Piton de la Fournaise waters wave low temperatures, ranging between 8.5 and 21.1 °C, and neutral pH values ranging between 6.5 and 8.6. Most samples also display low electrical conductivities, although five (TUN1, TUN2, TUN3, SPH3, SPI3) display values superior to the others (266 to 685 µS/cm against a mean of 129 ± 100 µS/cm, Supplementary Data 1 and Fig. 1B).

The mineralization of rainwaters, which infiltrate the volcanic edifice, is mostly influenced by sea spray and thus have a Na/Cl ratio close to that of seawater, with however low Na and Cl concentrations[36]. From this initial composition, as water circulates through the ground, its composition evolves according to different mineralization processes. In Fig. 1B, the comparison of Na/Cl and Na/NO_3 molar ratios gives three trends corresponding to three common mineralization processes: water-rock interaction, seawater contamination, and anthropogenic contamination. As the water residence time in the aquifers increases, water-rock interaction increases the Na concentration through the dissolution of silicate bearing minerals[36], giving the first trend. Additionally, seawater may contaminate samples collected at river mouths and in wells close to the coast (SPH2, SPH3, SPH4), increasing both Na and Cl concentrations[36], giving the

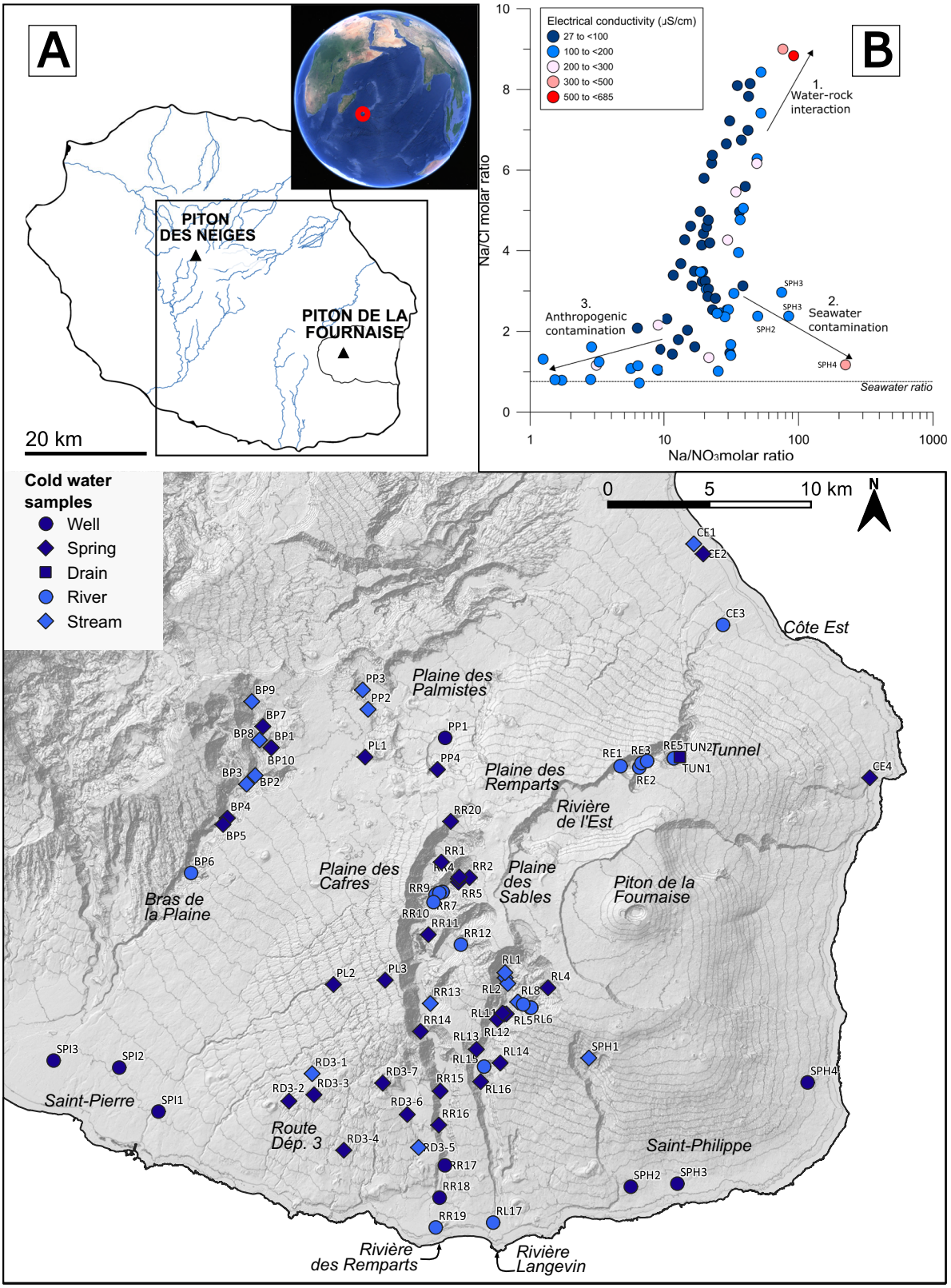

Fig. 1 Locations and main geochemical features of Piton de la Fournaise waters. A Map of the different water samples of Piton de la Fournaise collected for this study and (**B**) Na/Cl vs. Na/NO_3 molar ratios and electrical conductivity (µS/cm) of Piton de la Fournaise waters, showing that water rock interaction, anthropogenic contamination and seawater contamination are the main mineralization processes. Insert: ©2023 Google Earth.

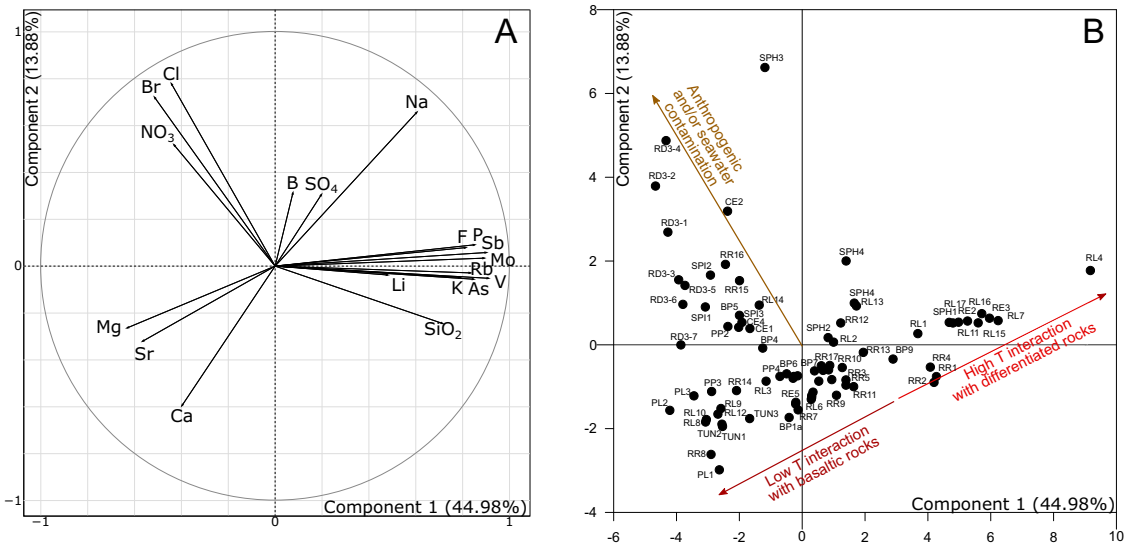

Fig. 2 Principal component analysis of the major and trace elements composition of Piton de la Fournaise waters. Distribution of (**A**) variables and (**B**) indices for components 1 and 2, representing 58.86% of the total variance.

second trend. Finally, the presence of urban areas and agricultural lands located on the catchment areas of several sampled watersheds can lead to the infiltration of artificially chlorinated waters from the domestic water supply, of organochlorine compounds and muckspreading used for agriculture and of wastewaters. These anthropogenic pollutions result increased Cl and NO_3 concentrations in waters, giving the third trend. The electrical conductivity of Piton de la Fournaise waters (blue to red scale, Fig. 1B), which is a proxy for their total dissolved mineral content, increases along each trend. This means that those three processes contribute the most to the geochemical composition of the waters. Here, we are searching for evidence of mineralization associated with hydrothermal processes. Seawater contamination and anthropogenic contamination are not hydrothermal processes. Water-rock interaction can occur at low temperature, but it is facilitated by heat and acidity, and can thus be increased by hydrothermal activity. However, from the data presented in Fig. 1B alone, it is not possible to decipher whether water-rock interaction evidenced here is associated with hydrothermal activity.

For a broader understanding of the geochemical composition of our samples, and in order to highlight a possible hydrothermal contribution, we performed a principal component analysis (PCA) on a large geochemical dataset of major and trace element compositions (variables) of our water samples from Piton de la Fournaise (individuals).

Among all of the analyzed elements, the variables retained for interpretation are:

Major elements (except HCO_3 for which not all samples had available data),
Trace elements that can originate from hydrothermal activity Li, B, Br, F, P, Sb, Mo, Rb, V, As, Sr,
SiO_2 as a maker of water rock interaction due to the weathering of silicate minerals[30,37],
NO_3 as a marker of anthropogenic contamination.

We did not include HCO_3 in the PCA because it requires a homogeneous dataset and HCO_3 concentrations had not been measured for some samples.

Using elemental concentrations for the PCA gives larger weights to the elements with the highest concentrations. Since in our case the hydrothermal component may not constitute the main geochemical feature, and since most elements associated with hydrothermal activity are trace elements, we chose to rather study the enrichment in each element compared to the others for each sample. To obtain this enrichment, we normalized the data by dividing each elemental concentration by the sum of the concentrations of the major cations (Ca, Mg, Na, K).

The results of the analysis are presented in Fig. 2A, B, which display the contribution of each chemical element to the two principal components, and the distribution of water samples on these components, respectively.

The first component explains 44.98% of the total geochemical variability. The elements contributing the most to this component are F, P, Sb, Mo, Rb, V, K, As, and to some extent SiO_2, Na and Li. F, P, Sb, Mo, Rb, V, K, As plot close together and define a pole. These chemical elements are found in magmatic gases, their condensates and associated deposits[38–41], as observed at Piton de la Fournaise[42,43], which can dissolve in waters. But in our case, F, P, Sb, Mo, Rb, V, K and As plot close to SiO_2, which is a marker of water-rock interaction, so we preferably explain their presence by a high temperature interaction with differentiated rocks[44–48], and thus by hydrothermal activity. By comparison, at the other volcano of La Réunion, Piton des Neiges, thermal springs display high concentrations in F, Rb, K, As and SiO_2 but not in V and P, and there is no available data for Mo and Sb[49]. Elements that can form oxyanions such as P, V, Mo and Sb have a higher solubility in oxidizing environments[47,50–52]. Therefore, they are more likely to be present in an unconfined aquifer such as in Piton de la Fournaise, especially at the top of the water column, where the conditions are more oxic.

The second component explains 13.88% of the total geochemical variability. The elements contributing the most to this component are Br, Cl, NO_3, Na and to some extent, B and SO_4. Br, Cl and NO_3 plot close together and define a second pole which we infer to be anthropogenic and/or seawater contamination.

A third pole can be identified on the negative end of both components, which corresponds to an enrichment in Mg, Ca and Sr. In the aquifers of Réunion Island, Ca and Mg are inferred to come from low temperature interaction with basaltic rocks[30], which we infer to be the main mineralization process for this third pole. However, an enrichment in magmatic gases can cause the pH to decrease and facilitate water-rock interaction.

Therefore, an enrichment in Mg, Ca and Sr could also be a knock-on effect of hydrothermal activity.

Na plots close to the circle and in-between the components 1 and 2, meaning it is contributing to both.

Elements Li, B and SO_4 are poorly represented on the two main components resulting from the PCA analysis (Fig. 2A), indicating that they originate from multiple sources. Sulfur species, Li and B are found in magmatic gases at Piton de la Fournaise[53,54] that could contribute to a hydrothermal system. Li and B can also come from high temperature interaction with differentiated rocks[45,55–57]. At Piton des Neiges volcano, previous studies show that several thermal springs and rivers streams contain high concentrations of Li, B, and SO_4 (up to 137.1 µmol/l, 1545.4 µmol/l and 8.28 mmol/l, respectively) with low δ^7Li and δ^{11}B values, which can be associated with hydrothermal activity[49,58,59]. At Piton de la Fournaise, as expected, Li, B, and SO_4 concentrations are several orders of magnitude lower than those of Piton des Neiges thermal springs. However, some samples display higher concentrations in these elements (up to 0.22 µmol/l, 14.92 µmol/l and 0.09 mmol/l, respectively) compared to all samples (median values: 0.02 µmol/l, 0.48 µmol/l and 0.01 mmol/l, respectively), which could correspond to a small hydrothermal contribution. Regarding the Li content of Piton de la Fournaise waters, it should be noted that Henchiri et al.[58] analyzed the composition in Li at two locations, the mouth of Rivière Langevin and the mouth of Rivière de l'Est. Samples were taken at the same locations for our study. The two studies show that the Li concentration is low: 0.032 and 0.009 µmol/l, respectively, in Henchiri et al.[58], and 0.021 and 0.025 µmol, respectively, in our study (Supplementary Data 1). Therefore, we do not consider these datapoints to be representative of the enriched Li pole with a possible hydrothermal input which we identified. Indeed, their δ^7Li values do not indicate a contribution from a hydrothermal source.

The hydrothermal contribution in boron can come from the dissolution of the host rock, of a magmatic gas phase or of fumarolic condensates or sublimates. Little fractionation is expected during these processes[60], and therefore, in any case the δ^{11}B value should be close to that of ocean island basalts (OIB). There are no available δ^{11}B values for Réunion basalts, but other OIB unaltered basalts display δ^{11}B values between −12 and −3‰[61]. Hydrothermal alteration or contamination by subducted slabs can increase these values. At Piton des Neiges volcano, where hydrothermal alteration is evidenced in the host rock[62], thermal springs have an isotopic ratio δ^{11}B comprised between 0.2 and 3.9‰ (this study[26]). At Piton de la Fournaise, where there is less hydrothermally altered rocks[62–64], the δ^{11}B value of the hydrothermal contribution should be lower, close to the basalt value. Additionally to a possible hydrothermal contribution, in groundwaters and river waters, boron is controlled by water-rock interaction at low temperature, by processes fractionating boron isotopes (mainly the sorption onto mineral and organic surfaces and coprecipitation of boron in secondary minerals, all favoring incorporation of isotope ^{10}B, and leaving the waters enriched in ^{11}B, so with higher δ^{11}B[65]), but also by the biological productivity, by the influence of sea spray in the infiltrated rainwater and by mixing with seawater. All of these other contributions are expected to result in natural waters displaying a higher δ^{11}B isotopic ratio than that of thermal waters (>12‰[65]). Therefore, the isotopic ratio δ^{11}B can be used to discriminate the hydrothermal contribution from these other sources of B in groundwaters and river waters[66–68]. Only anthropogenic contamination would possibly bring B with low δ^{11}B signatures, either issued from urban/industrial uses or from fertilizers[69–71]. Measured δ^{11}B values for Piton de la Fournaise waters range from −5.0 to 42.7‰ in agreement with previous values by Louvat et al.[58] (from 3.7 to 44.2‰). Nine samples out of the 28 for which δ^{11}B was analyzed display low δ^{11}B values (typically <12‰): TUN1, TUN2, TUN3, RL4, RL1, RE4, RR3, RL5 and RL3. These samples come from preserved natural environments, and do not show anthropogenic contamination according to their position in the principal component analysis plot (Fig. 2). Therefore, these waters are interpreted as being strongly influenced by a hydrothermal system.

CO_2 is the most abundant magmatic gas[72] and can dissolve in waters. Considering the pH (7.6 ± 0.4) and temperature (16.2 ± 2.6 °C) of the waters of Piton de la Fournaise, this dissolved carbon should be mostly in the form of HCO_3. The HCO_3 content can thus be an indicator of the presence of magmatic degassing. HCO_3 concentrations of Piton de la Fournaise waters range between 0.20 and 4.77 mmol/l. This upper value is in the range of Piton des Neiges thermal waters (3.1 to 42.7 mmol/l[49]), indicating that there is a probable magmatic source of carbon at Piton de la Fournaise. However, part of the dissolved carbon can also come from a biogenic source. The isotopic ratio δ^{13}C of the total dissolved inorganic carbon (TDIC) can be used to discriminate between a biogenic and a magmatic source of carbon. At Piton de la Fournaise, magmatic gaseous CO_2 is expected to have a δ^{13}C value comprised between −0.5 and −8‰[73–75]. Dissolution of this gaseous carbon in waters does not affect the isotopic ratio, but there is an isotopic fractionation if this CO_2 is lost through degassing from the water, resulting in higher values of δ^{13}C in the residual waters[49,74,76]. A biogenic contribution (through the respiration of micro-organisms in the soils and vegetation C use) results in lower values of δ^{13}C in waters ($\delta^{13}C \leq -20$ in Réunion[77]). For Piton de la Fournaise waters, we were only able to get δ^{13}C isotopic ratios for 54 out of 82 samples, the remaining samples having too low TDIC (see methods section). δ^{13}C values range between −21.4 and 0.6‰ (Supplementary Data 1). Fourteen samples display δ^{13}C values in the range of that of magmatic CO_2 and 3 have a clear biogenic signature. For the others, we infer that the carbon content is a mix between both sources. In Fig. 3, we represented the δ^{11}B and δ^{13}C values for the 25 samples for which both parameters were analyzed. Three samples display δ^{11}B and δ^{13}C in the range of the expected values for B and C originating from magmatic or hydrothermal activity, and several appear to tend toward this pole.

Piton de la Fournaise hydrothermal system revealed. From our geochemical study, we can retain several geochemical markers of hydrothermal activity: the relative enrichments in As, Rb, P, V, Mo, Sb, F, Li, SO_4 and B compared to other elements, the concentration in HCO_3 and the isotopic ratios δ^{11}B and δ^{13}C. These markers are found in several samples and in different proportions. In this section, we use these markers to compare the hydrothermal contributions in the different samples.

Each of the markers (Y) can be converted to a linear scale from 0 to 1 (index Y_i) measuring the relative likelihood of the presence of a hydrothermal component (Table 1). Depending on the elements, additional operations can be made to account for the influence of the dilution of the hydrothermal fluid and of seawater and anthropogenic contaminations.

The enrichments in As, Rb, P, V, Mo, Sb and F, Li, SO_4 and B are obtained by dividing the elemental concentrations by the sum of the major cations, which approximates the total mineral content. This corrects for both dilution of hydrothermal fluids and seawater contamination, as both affect the global geochemical composition of waters. SO_4 and B concentrations can be affected also by anthropogenic contamination, which only partially affect

the global geochemical composition. Therefore, here, we correct for anthropogenic contamination by also dividing the SO_4 and B concentrations by the NO_3 concentration (Table 1).

HCO_3 concentration can be affected by dilution. However, this compound is inferred to originate from CO_2 dissolution, which promotes mineral dissolution and in turn increases the total mineral content. Hence, HCO_3 concentration cannot be corrected for dilution.

While elemental concentrations of B and HCO_3 give a relative probability of the presence of a hydrothermal component of each water sample compared to the others, isotopic ratios $\delta^{11}B$ and $\delta^{13}C$ can be considered as absolute linear scales. The maximum likelihood of the presence of a hydrothermal component corresponds to the highest value for $\delta^{13}C$ and to the lowest value for $\delta^{11}B$, resulting in an inverse scale (Table 1).

We use these indexes Y_i to build a global hydrothermal index (HI = Hydrothermal Index, Eq. (1)). All indexes Y_i are normalized between 0 and 1, weighted and summed (Table 1). From the result of the PCA, we know that As, Rb, P, V, Mo, Sb and F are representative of a unique hydrothermal process. Therefore, their 7 indexes Y_i are summed, and each is given a weight of 1/7. Other indexes are each given a weight of 1. The hydrothermal index is then computed with the following equation:

$$HI = \frac{\frac{As_i+Rb_i+P_i+V_i+Mo_i+Sb_i+F_i}{7} + SO_{4,i} + B_i + Li_i + HCO_{3,i} + \delta^{11}B_i + \delta^{13}C_i}{n} \quad (1)$$

where n corresponds to the number of terms of the numerator. $\delta^{11}B$ and/or $\delta^{13}C$ were not analyzed for all samples. As a result, n equals at least 5 and at most 7. We then normalized the hydrothermal index between 0 and 1, giving the number HI_{norm}.

The spatial distribution of the values of the normalized hydrothermal index HI_{norm} in Piton de la Fournaise waters is represented in Fig. 4, along with major geological features that can constitute preferential pathways for hydrothermal fluids or heat sources: caldera faults[78], rift zones[79] dense bodies and conductive layers[9]. The waters most likely to have a hydrothermal component ($HI_{norm} > 0.5$) are all located on or close to the caldera faults surrounding the Plaine des Sables region, except for four of them (wells SPH2, SPH3, SPH4 and spring RL15). However, these four samples drain an aquifer which can be considered continuous from the Summit/Plaine des Sables region down to the shore[30,80], meaning that their geochemical composition could be inherited from upstream. This spatial distribution indicates that the caldera faults act as preferential pathways for rising hydrothermal fluids. In La Plaine des Sables region, located at the center of this caldera fault system, a dense body and a conductive layer have already been identified as a possible geothermal resource (Fig. 4). Our study provides additional evidence in favor of this interpretation. Therefore, la Plaine des Sables can be considered the best target for geothermal exploration in terms of geothermal potential. This

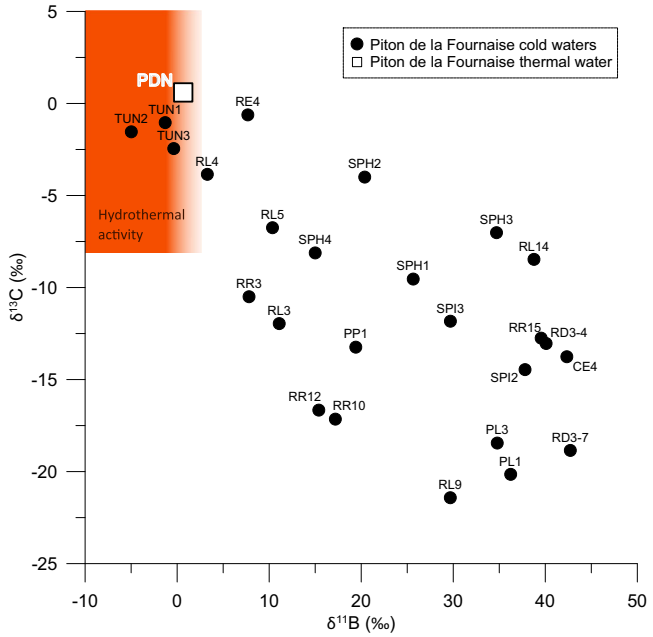

Fig. 3 $\delta^{11}B$ and $\delta^{13}C$ isotopic ratios of Piton de la Fournaise waters compared to a thermal water sample from Piton des Neiges. The expected ranges for boron and carbon originating from hydrothermal activity are also represented by the red field[14,34,49,53,55–57].

Table 1 Geochemical markers of hydrothermal activity converted as indexes measuring the likelihood of the presence of a hydrothermal component.

Marker Y	Index Y_i	Corrections	Weight
[As]	$As_i = \frac{[As]}{[Ca]+[Mg]+[Na]+[K]}$, normalized between 0 and 1	Dilution, Seawater contamination	1/7
[Rb]	$Rb_i = \frac{[Rb]}{[Ca]+[Mg]+[Na]+[K]}$, normalized between 0 and 1		1/7
[P]	$P_i = \frac{[P]}{[Ca]+[Mg]+[Na]+[K]}$, normalized between 0 and 1		1/7
[V]	$V_i = \frac{[V]}{[Ca]+[Mg]+[Na]+[K]}$, normalized between 0 and 1		1/7
[Mo]	$Mo_i = \frac{[Mo]}{[Ca]+[Mg]+[Na]+[K]}$, normalized between 0 and 1		1/7
[Sb]	$Sb_i = \frac{[Sb]}{[Ca]+[Mg]+[Na]+[K]}$, normalized between 0 and 1		1/7
[F]	$F_i = \frac{[F]}{[Ca]+[Mg]+[Na]+[K]}$, normalized between 0 and 1		1/7
[Li]	$Li_i = \frac{[Li]}{[Ca]+[Mg]+[Na]+[K]}$, normalized between 0 and 1		1
$[SO_4]$	$SO_{4,i} = \frac{[SO_4]/[NO_3]}{[Ca]+[Mg]+[Na]+[K]}$, normalized between 0 and 1	Dilution, Seawater contamination, Anthropogenic contamination	1
[B]	$B_i = \frac{[B]/[NO_3]}{[Ca]+[Mg]+[Na]+[K]}$, normalized between 0 and 1		1
$[HCO_3]$	$HCO_{3,i} = [HCO_3]$, normalized between 0 and 1		1
$\delta^{11}B$	$\delta^{11}B_i = 1/\delta^{11}B$, normalized between 0 and 1		1
$\delta^{13}C$	$\delta^{13}C_i = \delta^{13}C$, normalized between 0 and 1		1

These indexes correct for other possible origins of these elements as well as for dilution. Each index is normalized between 0 and 1 and given a weight to compute a global index.

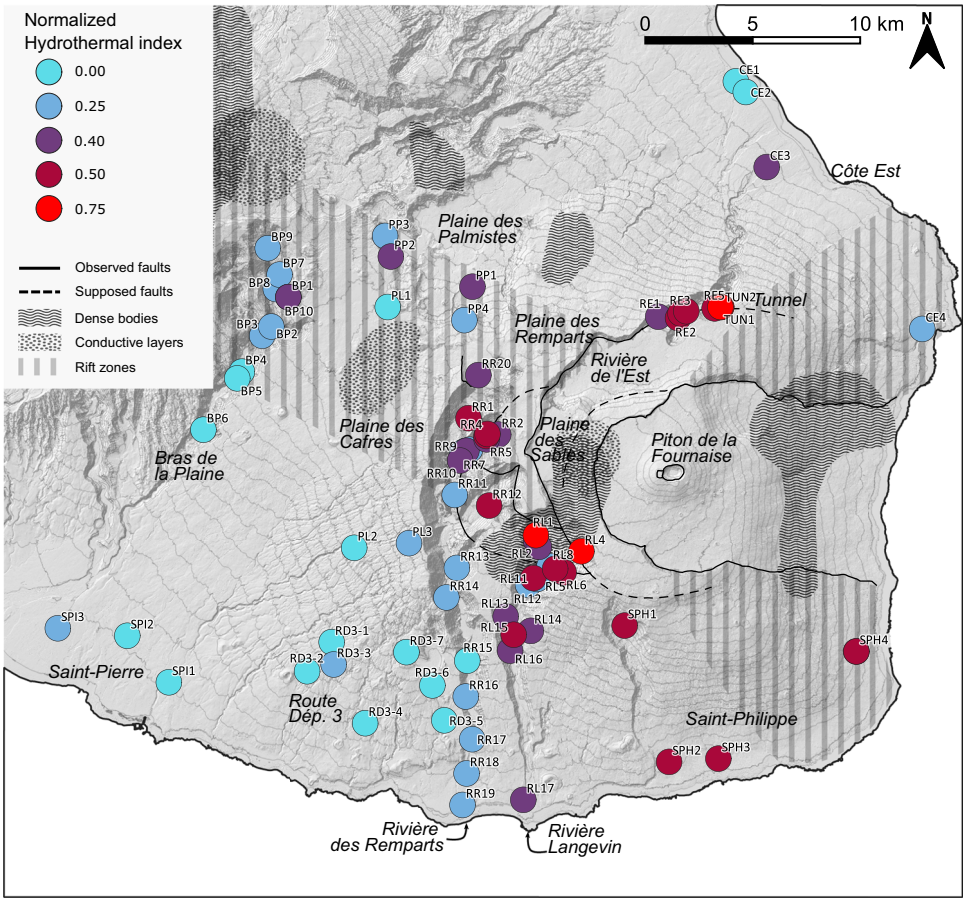

Fig. 4 Spatial distribution of the normalized hydrothermal index, indicating the relative probability of the presence of a hydrothermal component in the waters of Piton de la Fournaise. Geological, structural and geophysical features are also represented: caldera faults[78], rift zones[79] dense bodies and conductive layers[24,28,29].

region has exceptional landscapes and biodiversity, and as such is part of a national park and is a UNESCO World heritage site, protected by strict environmental regulations, which any geothermal project will need to account for.

Our study demonstrates that the geochemistry of cold waters is an efficient way to address the first stage of geothermal exploration in blind systems, which is to determine whether or not there is hydrothermal activity generating energy at depth, and it proves to be complementary to other approaches. Regardless of the extent of the contribution of hydrothermal activity to the geochemical composition of waters, as long as it exists, the study of relevant elemental and isotopic ratios can highlight it. Spatializing this diffuse hydrothermal signal points to geographical and structural targets for geothermal exploration.

Methods

The groundwaters and surface waters of Piton de la Fournaise were sampled during the dry season in 2020 and 2021, when the water tables are at a low level, in an effort to minimize mixing with newly infiltrated rainfall. These campaigns yielded a total of 82 water samples (from 80 sampling points) to be analyzed for major and trace elements concentrations and $\delta^{13}C$ and $\delta^{11}B$ isotopic ratios. The pH, temperature, and electrical conductivity (EC, expressed at 25 °C) of each sample were measured in situ. All water samples were filtered at 0.2 µm on site and the containers were rinsed three times with filtered water. Samples for the analysis of major, trace elements and B isotopes were collected in LDPE bottles. Samples for the analysis of major cations and trace elements were acidified with nitric acid (HNO_3 0.6 N) on site. Samples for the analysis of total dissolved inorganic carbon content (TDIC) and C isotopes were collected in Labco 12 ml Exetainer vials with no headspace. All samples were stored at a temperature of 6 °C before shipment.

All analyses were performed at the Institut de Physique du Globe de Paris (IPGP). Major anions, fluoride and nitrate concentrations were determined by ion exchange chromatography. Major cations and trace element concentrations were determined using inductively coupled plasma mass spectrometry (ICP-MS). The accuracy for major cations and anions concentrations is <5%, and <20% for trace elements, as inferred from replicate measurement of solutions of known compositions. The TDIC and carbon isotope ratios of the TDIC were determined together by gas chromatography and isotope ratio mass spectrometry (GC-IRMS), after releasing the TDIC as CO_2 by H_3PO_4 acidification in a vial from an aliquot of 5 ml[81]. For the analysis with the GC-IRMS, a finite amount of gas is pumped inside the vial and sent into the analysis circuit. This step is repeated several times and the TDIC and $\delta^{13}C$ are computed from the results of several runs. This method proved not adapted for the analysis of our samples due to a too low content of TDIC. With an aliquot of just 5 ml, the available gaseous CO_2 in the vial sampled by the GC-IRMS was too low and the analysis did not yield results for several runs and for several samples. We obtained reliable results for only 51 out of 82 samples. For these samples, HCO_3 concentrations were computed from TDIC, pH and temperature, using the temperature dependent acid dissociation constants from Mook and Koene, (1975)[82]. For the other samples, HCO_3 concentrations were estimated for an ionic balance equal to 0%. $\delta^{13}C$ are

reported relative to PDB standard with a 1 SD reproducibility, ±0.05‰. Boron isotope ratios were determined by MC-ICP-MS with a direct injection nebulizer (d-DIHEN[83]), after boron extraction through ion chromatography[84]. $\delta^{11}B$ are reported relative to NIST SRM951 standard with a 2 SD reproducibility, between 0.1 and 0.4‰.

Data availability

The data used in this manuscript are available as Supplementary Data and also through IPGP Research Collection (research-collection.ipgp.fr) at the following https://doi.org/10.18715/IPGP.2023.lq6ndlzz[85].

Received: 15 May 2023; Accepted: 9 January 2024;
Published online: 29 January 2024

References

1. Faulds, J. & Hinz, N. Favorable tectonic and structural settings of geothermal systems in the Great Basin region, western USA: proxies for discovering blind geothermal systems. In *Proceedings World Geothermal Congress, Melbourne, Australia* (2015).
2. Fercho, S. et al. Blind geothermal system exploration in active volcanic environments; multi-phase geophysical and geochemical surveys in overt and subtle volcanic systems, Hawai'i and Maui. https://www.osti.gov/biblio/1242411; https://doi.org/10.2172/1242411 (2015).
3. Lautze, N. et al. Play fairway analysis of geothermal resources across the State of Hawaii: 1. Geological, geophysical, and geochemical datasets. *Geothermics* **70**, 376–392 (2017).
4. Lewicki, J. L. & Oldenburg, C. M. Stragegies to detect hidden geothermal systems based on monitoring and analysis of CO_2 in the near-surface environment. *Geophysical Research Letter* 32, (LBNL-57414) (2008).
5. Lewicki, J. L. & Oldenburg, C. M. Near-surface CO_2 monitoring and analysis to detect hidden geothermal systems. *Thirtieth Workshop on Geothermal Reservoir Engineering, Stanford, CA (US)*. 2005, (LBNL-56900) (2005).
6. Voltattorni, N., Sciarra, A. & Quattrocchi, F. The application of soil gas technique to geothermal exploration: study of "hidden" potential geothermal systems. In: *World Geothermal Congress 2010 (WGC2010)* (2010).
7. Wannamaker, P. E., Faulds, J. E. & Kennedy, B. M. *Integrating Magnetotellurics, Soil Gas Geochemistry and Structural Analysis to Identify Hidden, High Enthalpy, Extensional Geothermal Systems*. https://www.osti.gov/biblio/1457571; https://doi.org/10.2172/1457571 (2017).
8. Louvat, P. & Allègre, C. J. Present denudation rates on the island of Réunion determined by river geochemistry: basalt weathering and mass budget between chemical and mechanical erosions. *Geochim. Cosmochim. Acta* **61**, 3645–3669 (1997).
9. Louvat, P. & Allègre, C. J. Riverine erosion rates on Sao Miguel volcanic island, Azores archipelago. *Chem. Geol.* **148**, 177–200 (1998).
10. Rad, S. D., Allègre, C. J. & Louvat, P. Hidden erosion on volcanic islands. *Earth Planet. Sci. Lett.* **262**, 109–124 (2007).
11. Louvat, P., Gislason, S. R. & Allègre, C. J. Chemical and mechanical erosion rates in Iceland as deduced from river dissolved and solid material. *Am. J. Sci.* **308**, 679–726 (2008).
12. Dessert, C., Gaillardet, J., Dupre, B., Schott, J. & Pokrovsky, O. S. Fluxes of high- versus low-temperature water–rock interactions in aerial volcanic areas: example from the Kamchatka Peninsula, Russia. *Geochim. Cosmochim. Acta* **73**, 148–169 (2009).
13. Gaillardet, J. et al. Orography-driven chemical denudation in the Lesser Antilles: evidence for a new feed-back mechanism stabilizing atmospheric CO_2. *Am. J. Sci.* **311**, 851–894 (2011).
14. Freire, P., Andrade, C., Coutinho, R. & Cruz, J. V. Fluvial geochemistry in São Miguel Island (Azores, Portugal): source and fluxes of inorganic solutes in an active volcanic environment. *Sci. Total Environ.* **454–455**, 154–169 (2013).
15. Rivé, K., Gaillardet, J., Agrinier, P. & Rad, S. Carbon isotopes in the rivers from the Lesser Antilles: origin of the carbonic acid consumed by weathering reactions in the Lesser Antilles. *Earth Surf. Process. Landf.* **38**, 1020–1035 (2013).
16. Hosono, T. et al. Earthquake-induced structural deformations enhance long-term solute fluxes from active volcanic systems. *Sci. Rep.* **8**, 14809 (2018).
17. Romero-Mujalli, G. et al. Hydrothermal and magmatic contributions to surface waters in the Aso caldera, southern Japan: implications for weathering processes in volcanic areas. *Chem. Geol.* **588**, 120612 (2022).
18. Gaspard, F. et al. Imprint of chemical weathering and hydrothermalism on the Ge/Si ratio and Si isotope composition of rivers in a volcanic tropical island, Basse-Terre, Guadeloupe (French West Indies). *Chem. Geol.* **577**, 120283 (2021).
19. Gaspard, F. et al. Quantifying non-thermal silicate weathering using Ge/Si and Si isotopes in rivers draining the Yellowstone Plateau Volcanic Field, USA. *Geochem. Geophys. Geosystems* **22**, e2021GC009904 (2021).
20. Schopka, H. H., Derry, L. A. & Arcilla, C. A. Chemical weathering, river geochemistry and atmospheric carbon fluxes from volcanic and ultramafic regions on Luzon Island, the Philippines. *Geochim. Cosmochim. Acta* **75**, 978–1002 (2011).
21. Hurwitz, S., Evans, W. C. & Lowenstern, J. B. River solute fluxes reflecting active hydrothermal chemical weathering of the Yellowstone Plateau Volcanic Field, USA. *Chem. Geol.* **276**, 331–343 (2010).
22. Carey, A. E. et al. Assessment of stream geochemistry in west central Nicaragua during baseflow conditions. *Appl. Geochem.* **63**, 519–526 (2015).
23. Ferguson, C. M. *Exploration for Blind Geothermal Resources in the State of Hawai'i Utilizing Dissolved Noble Gasses in Well Waters* (University of Hawai'i, 2020).
24. Dezayes, C., Famin, V., Tourlière, B., Baltassat, J.-M. & Bénard, B. Potential areas of interest for the development of geothermal energy in La Réunion Island based on GIS analysis. *J. Volcanol. Geotherm. Res.* **421**, 107450 (2022).
25. Basseguy, S. *Étude du Signal Hydrogéologique du Radon des Eaux Souterraines de l'Île de la Réunion* (Université de La Réunion, 2008).
26. Louvat, P., Gayer, E. & Gaillardet, J. Boron behavior in the rivers of Réunion island, inferred from boron isotope ratios and concentrations of major and trace elements. *Procedia Earth Planet. Sci.* **10**, 231–237 (2014).
27. Nicolini, E., Olive, P., Coudray, J. & Jusserand, C. Circulation des eaux dans le massif du Piton de la Fournaise (Ile de la Réunion) et leur contamination par des fluides d'origine magmatique. *C. R. Acad. Sci.* **312**, 535–542 (1991).
28. PB Power. *'Projet Géothermie Réunion' Campagne MT/TDEM 2004. Rapport global de synthèse* (2005).
29. PB Power. *'Projet Géothermie Réunion' Rapport Global de synthèse* (2003).
30. Join, J.-L., Folio, J.-L., Bourhane, A. & Comte, J.-C. Groundwater resources on active basaltic volcanoes: conceptual models from La Réunion Island and Grande Comore. in *Active Volcanoes of the Southwest Indian* Ocean (eds Bachelery, P., Lenat, J.-F., Di Muro, A. & Michon, L.) 61–70 (Springer, 2016).
31. Famin, V., Welsch, B., Okumura, S., Bachèlery, P. & Nakashima, S. Three differentiation stages of a single magma at Piton de la Fournaise volcano (Reunion hot spot). *Geochem. Geophys. Geosyst.* **10** https://doi.org/10.1029/2008GC002015 (2009).
32. Upton, B. G. J. & Wadsworth, W. J. The basalts of Réunion Island, Indian Ocean. *Bull. Volcanol.* **29**, 7–23 (1966).
33. Albarede, F. & Tamagnan, V. Modelling the recent geochemical evolution of the Piton de la Fournaise Volcano, Reunion Island, 1931–1986*. *J. Petrol.* **29**, 997–1030 (1988).
34. Dumont, M. *Caractérisation Multi-échelle des Structures Hydrogéologiques en Contexte Volcanique Insulaire par Électromagnétisme Héliporté: Application à l'île de La Réunion* (La Réunion, 2018).
35. Dumont, M. et al. Hydrogeophysical characterization in a volcanic context from local to regional scales combining airborne electromagnetism and magnetism. *Geophys. Res. Lett.* **48**, e2020GL092000 (2021).
36. Join, J.-L., Coudray, J. & Longworth, K. Using principal components analysis and Na/Cl ratios to trace groundwater circulation in a volcanic island: the example of Reunion. *J. Hydrol.* **190**, 1–18 (1997).
37. Clark, I. *Groundwater Geochemistry and Isotopes* (CRC Press, 2015).
38. Africano, F., Van Rompaey, G., Bernard, A. & Le Guern, F. Deposition of trace elements from high temperature gases of Satsuma-Iwojima volcano. *Earth Planets Space* **54**, 275–286 (2002).
39. Aiuppa, A., Parello, F., Allard, P., D'Alessandro, W. & Michel, A. Trace element hydrogeochemistry of Mt. Etna, Sicily: insight on water-rock interaction. in *Water-Rock Interaction* 195–198 (1998).
40. Ostroumov, M. & Taran, Y. Vanadium, V—a new native element mineral from the Colima volcano, State of Colima, Mexico, and implications for fumarole gas composition. *Mineral. Mag.* **80**, 371–382 (2016).
41. Sainlot, N. et al. Uptake of gaseous thallium, tellurium, vanadium and molybdenum into anhydrous alum, Lascar volcano fumaroles, Chile. *Geochim. Cosmochim. Acta* **275**, 64–82 (2020).
42. Gannoun, A., Vlastélic, I. & Schiano, P. Escape of unradiogenic osmium during sub-aerial lava degassing: evidence from fumarolic deposits, Piton de la Fournaise, Réunion Island. *Geochim. Cosmochim. Acta* **166**, 312–326 (2015).
43. Vlastélic, I. et al. Lead isotopes behavior in the fumarolic environment of the Piton de la Fournaise volcano (Réunion Island). *Geochim. Cosmochim. Acta* **100**, 297–314 (2013).
44. Arnórsson, S. & Óskarsson, N. Molybdenum and tungsten in volcanic rocks and in surface and <100 °C ground waters in Iceland. *Geochim. Cosmochim. Acta* **71**, 284–304 (2007).
45. Kaasalainen, H. & Stefánsson, A. The chemistry of trace elements in surface geothermal waters and steam, Iceland. *Chem. Geol.* **330–331**, 60–85 (2012).

46. Morales-Arredondo, I., Rodríguez, R., Armienta, M. A. & Villanueva-Estrada, R. E. The origin of groundwater arsenic and fluorine in a volcanic sedimentary basin in central Mexico: a hydrochemistry hypothesis. *Hydrogeol. J.* **24**, 1029–1044 (2016).
47. Rango, T., Vengosh, A., Dwyer, G. & Bianchini, G. Mobilization of arsenic and other naturally occurring contaminants in groundwater of the Main Ethiopian Rift aquifers. *Water Res.* **47**, 5801–5818 (2013).
48. Stefánsson, A. & Arnórsson, S. The geochemistry of As, Mo, Sb, and W in natural geothermal waters, Iceland. in *Proceedings of the World Geothermal Congress*, *Antalya, Turkey* 24–29 (Citeseer, 2005).
49. Bénard, B. et al. Origin and fate of hydrothermal fluids at Piton des Neiges volcano (Réunion Island): a geochemical and isotopic (O, H, C, Sr, Li, Cl) study of thermal springs. *J. Volcanol. Geotherm. Res.* **392**, 106682 (2020).
50. Aiuppa, A. et al. Mobility and fluxes of major, minor and trace metals during basalt weathering and groundwater transport at Mt. Etna volcano (Sicily). *Geochim. Cosmochim. Acta* **64**, 1827–1841 (2000).
51. Cinti, D. et al. Spatial distribution of arsenic, uranium and vanadium in the volcanic-sedimentary aquifers of the Vicano–Cimino Volcanic District (Central Italy). *J. Geochem. Explor.* **152**, 123–133 (2015).
52. Wehrli, B. & Stumm, W. Vanadyl in natural waters: adsorption and hydrolysis promote oxygenation. *Geochim. Cosmochim. Acta* **53**, 69–77 (1989).
53. Di Muro, A. et al. Magma degassing at Piton de la Fournaise Volcano. in *Active Volcanoes of the Southwest Indian Ocean* 203–222 (Springer, 2016).
54. Vlastélic, I. et al. Lithium isotope fractionation during magma degassing: constraints from silicic differentiates and natural gas condensates from Piton de la Fournaise volcano (Réunion Island). *Chem. Geol.* https://doi.org/10.1016/j.chemgeo.2011.02.002 (2011).
55. Cullen, J. T., Barnes, J. D., Hurwitz, S. & Leeman, W. P. Tracing chlorine sources of thermal and mineral springs along and across the Cascade Range using halogen concentrations and chlorine isotope compositions. *Earth Planet. Sci. Lett.* **426**, 225–234 (2015).
56. Reyes, A. G. & Trompetter, W. J. Hydrothermal water–rock interaction and the redistribution of Li, B and Cl in the Taupo Volcanic Zone, New Zealand. *Chem. Geol.* **314–317**, 96–112 (2012).
57. Shaw, D. M. & Sturchio, N. C. Boron-lithium relationships in rhyolites and associated thermal waters of young silicic calderas, with comments on incompatible element behaviour. *Geochim. Cosmochim. Acta* **56**, 3723–3731 (1992).
58. Henchiri, S. et al. The influence of hydrothermal activity on the Li isotopic signature of rivers draining volcanic areas. *Procedia Earth Planet. Sci.* **10**, 223–230 (2014).
59. Sanjuan, B., Genter, A., Brach, M. & Lebon, D. *Compléments d'étude géothermique dans l'île de la Réunion (géologie, géochimie)*. 196 (2001).
60. Wu, S.-F., You, C.-F., Lin, Y.-P., Valsami-Jones, E. & Baltatzis, E. New boron isotopic evidence for sedimentary and magmatic fluid influence in the shallow hydrothermal vent system of Milos Island (Aegean Sea, Greece). *J. Volcanol. Geotherm. Res.* **310**, 58–71 (2016).
61. Marschall, H. R. Boron isotopes in the ocean floor realm and the mantle. in *Boron Isotopes: The Fifth Element* (eds Marschall, H. & Foster, G.) 189–215 (Springer International Publishing, 2018).
62. Gailler, L.-S. & Lénat, J.-F. Internal architecture of La Réunion (Indian Ocean) inferred from geophysical data. *J. Volcanol. Geotherm. Res.* **221–222**, 83–98 (2012).
63. Famin, V. et al. Localization of magma injections, hydrothermal alteration, and deformation in a volcanic detachment (Piton des Neiges, La Réunion). *J. Geodyn.* **101**, 155–169 (2016).
64. Lénat, J.-F., Bachèlery, P. & Merle, O. Anatomy of Piton de la Fournaise volcano (La Réunion, Indian Ocean). *Bull. Volcanol.* **74**, 1945–1961 (2012).
65. Gaillardet, J. & Lemarchand, D. Boron in the weathering environment. in *Boron Isotopes: The Fifth Element* (eds Marschall, H. & Foster, G.) 163–188 (Springer International Publishing, 2018).
66. Aggarwal, J. K. et al. The boron isotope systematics of Icelandic geothermal waters: 1. Meteoric water charged systems. *Geochim. Cosmochim. Acta* **64**, 579–585 (2000).
67. Louvat, P., Gaillardet, J., Paris, G. & Dessert, C. Boron isotope ratios of surface waters in Guadeloupe, Lesser Antilles. *Appl. Geochem.* **26**, S76–S79 (2011).
68. Millot, R., Hegan, A. & Négrel, P. Geothermal waters from the Taupo Volcanic Zone, New Zealand: Li, B and Sr isotopes characterization. *Appl. Geochem.* **27**, 677–688 (2012).
69. Guinoiseau, D. et al. Are boron isotopes a reliable tracer of anthropogenic inputs to rivers over time? *Sci. Total Environ.* **626**, 1057–1068 (2018).
70. Briand, C. et al. Legacy of contaminant N sources to the NO3− signature in rivers: a combined isotopic (δ15N-NO3−, δ18O-NO3−, δ11B) and microbiological investigation. *Sci. Rep.* **7**, 41703 (2017).
71. Widory, D. et al. Improving the management of nitrate pollution in water by the use of isotope monitoring: the δ15N, δ18O and δ11B triptych. *Isotopes Environ. Health Stud.* **49**, 29–47 (2013).
72. Edmonds, M. & Woods, A. W. Exsolved volatiles in magma reservoirs. *J. Volcanol. Geotherm. Res.* **368**, 13–30 (2018).
73. Boudoire, G., Rizzo, A. L., Di Muro, A., Grassa, F. & Liuzzo, M. Extensive CO2 degassing in the upper mantle beneath oceanic basaltic volcanoes: first insights from Piton de la Fournaise volcano (La Réunion Island). *Geochim. Cosmochim. Acta* **235**, 376–401 (2018).
74. Marty, B., Meynier, V., Nicolini, E., Griesshaber, E. & Toutain, J. P. Geochemistry of gas emanations: a case study of the Réunion Hot Spot, Indian Ocean. *Appl. Geochem.* **8**, 141–152 (1993).
75. Trull, T., Nadeau, S., Pineau, F., Polve´, M. & Javoy, M. C-He systematics in hotspot xenoliths: implications for mantle carbon contents and carbon recycling. *Earth Planet. Sci. Lett.* **118**, 43–64 (1993).
76. Ruzié, L. et al. Carbon and helium isotopes in thermal springs of La Soufrière volcano (Guadeloupe, Lesser Antilles): implications for volcanological monitoring. *Chem. Geol.* **359**, 70–80 (2013).
77. Liuzzo, M. et al. New evidence of CO2 soil degassing anomalies on Piton de la Fournaise volcano and the link with volcano tectonic structures. *Geochem. Geophys. Geosyst.* **16**, 4388–4404 (2015).
78. Merle, O., Mairine, P., Michon, L., Bachèlery, P. & Smietana, M. Calderas, landslides and paleo-canyons on Piton de la Fournaise volcano (La Réunion Island, Indian Ocean). *J. Volcanol. Geotherm. Res.* **189**, 131–142 (2010).
79. Michon, L., Ferrazzini, V. & Di Muro, A. Magma paths at Piton de la Fournaise Volcano. in *Active Volcanoes of the Southwest Indian Ocean: Piton de la Fournaise and Karthala* (eds Bachelery, P., Lenat, J.-F., Di Muro, A. & Michon, L.) 91–106 (Springer, 2016).
80. Folio, J.-L. *Distribution de la Perméabilité dans le Massif du Piton de la Fournaise: Apport à la Connaissance du Fonctionnement Hydrogéologique d'un Volcan-bouclier* (Université de La Réunion, 2001).
81. Assayag, N., Rivé, K., Ader, M., Jézéquel, D. & Agrinier, P. Improved method for isotopic and quantitative analysis of dissolved inorganic carbon in natural water samples. *Rapid Commun. Mass Spectrom.* **20**, 2243–2251 (2006).
82. Mook, W. G. & Koene, B. K. S. Chemistry of dissolved inorganic carbon in estuarine and coastal brackish waters. *Estuar. Coast. Mar. Sci.* **3**, 325–336 (1975).
83. Louvat, P. et al. A fully automated direct injection nebulizer (d-DIHEN) for MC-ICP-MS isotope analysis: application to boron isotope ratio measurements. *J. Anal. At. Spectrom.* **29**, 1698–1707 (2014).
84. Lemarchand, D., Gaillardet, J., Göpel, C. & Manhès, G. An optimized procedure for boron separation and mass spectrometry analysis for river samples. *Chem. Geol.* **182**, 323–334 (2002).
85. Bénard, B. et al. Location, physio-chemistry, geochemical composition of Piton de la Fournaise cold waters, and index probability (HInorm) of the presence of a hydrothermal component. https://doi.org/10.18715/IPGP.2023.lq6ndlzz (2023).

Acknowledgements

We thank Alix Marianne, Chris Payet and Manaarii Salmon for their participation in the fieldwork. The Communauté d'Agglomération du Sud de La Réunion (CASUD) funded the postdoctoral fellowship of Bhavani Bénard and this research. Chemical analyses were also supported by IPGP multidisciplinary program PARI and Paris–IdF region SESAME (Grant no. 12015908).

Author contributions

Bhavani Bénard contributed to all aspects of the project and wrote the article. Vincent Famin supervised the project, took part in the field work and data interpretation, and contributed to writing the article. Pierre Agrinier and Pascale Louvat conducted some of the analytical work of this project and contributed to interpreting the data and writing the article. Geneviève Lebeau contributed to the conceptualization and execution of the field work. Pierre Burckel conducted some of the analytical work of this project.

Competing interests

The authors declare no competing interests.

Additional information

Supplementary information The online version contains supplementary material available at https://doi.org/10.1038/s43247-024-01210-3.

Correspondence and requests for materials should be addressed to Bhavani Bénard.

Peer review information *Communications Earth & Environment* thanks the anonymous reviewers for their contribution to the peer review of this work. Primary Handling Editors: Lucia Pappalardo and Joe Aslin. A peer review file is available.